doi:10.1016/j.jmb.2012.04.005 J. Mol. Biol. (2012) 420, 87–98

Contents lists available at www.sciencedirect.com

Journal of Molecular Biology

journal homepage: http://ees.elsevier.com.jmb

Impacts of Dystrophin and Utrophin Domains on Actin Structural Dynamics: Implications for Therapeutic Design

Ava Yun Lin, Ewa Prochniewicz, Davin M. Henderson, Bin Li, James M. Ervasti and David D. Thomas*

Department of Biochemistry, Molecular Biology, and Biophysics, University of Minnesota, 6-155 Jackson Hall, 321 Church Street SE, Minneapolis, MN 55455, USA

Received 27 January 2012; received in revised form 26 March 2012; accepted 2 April 2012
Available online 11 April 2012

Edited by R. Craig

Keywords:
time-resolved phosphorescence anisotropy; TPA; muscular dystrophy; gene therapy

We have used time-resolved phosphorescence anisotropy (TPA) of actin to evaluate domains of dystrophin and utrophin, with implications for gene therapy in muscular dystrophy. Dystrophin and its homolog utrophin bind to cytoskeletal actin to form mechanical linkages that prevent muscular damage. Because these proteins are too large for most gene therapy vectors, much effort is currently devoted to smaller constructs. We previously used TPA to show that both dystrophin and utrophin have a paradoxical effect on actin rotational dynamics—restricting amplitude while increasing rate, thus increasing resilience, with utrophin more effective than dystrophin. Here, we have evaluated individual domains of these proteins. We found that a "mini-dystrophin," lacking one of the two actin-binding domains, is less effective than dystrophin in regulating actin dynamics, correlating with its moderate effectiveness in rescuing the dystrophic phenotype in mice. In contrast, we found that a "micro-utrophin," with more extensive internal deletions, is as effective as full-length dystrophin in the regulation of actin dynamics. Each of utrophin's actin-binding domains promotes resilience in actin, while dystrophin constructs require the presence of both actin-binding domains and the C-terminal domain for full function. This work supports the use of a utrophin template for gene or protein therapy designs. Resilience of the actin–protein complex, measured by TPA, correlates remarkably well with previous reports of functional rescue by dystrophin and utrophin constructs in *mdx* mice. We propose the use of TPA as an *in vitro* method to aid in the design and testing of emerging gene therapy constructs.

Introduction

Duchenne and Becker muscular dystrophies are caused by mutations in dystrophin, a 427-kDa protein localized to the cytoskeletal lattice of the sarcolemma.[1] Dystrophin's N-terminus binds to cytoskeletal actin, and the C-terminus (CT) binds to the dystroglycoprotein complex at the sarcolemma membrane (Fig. 1). Lack of functional dystrophin in skeletal muscles results in disarray of the

*Corresponding author. E-mail address: ddt@umn.edu.

Abbreviations used: TPA, time-resolved phosphorescence anisotropy; STR, spectrin-type repeat; wt, wild type; ErIA, erythrosine iodoacetamide; NIH, National Institutes of Health.

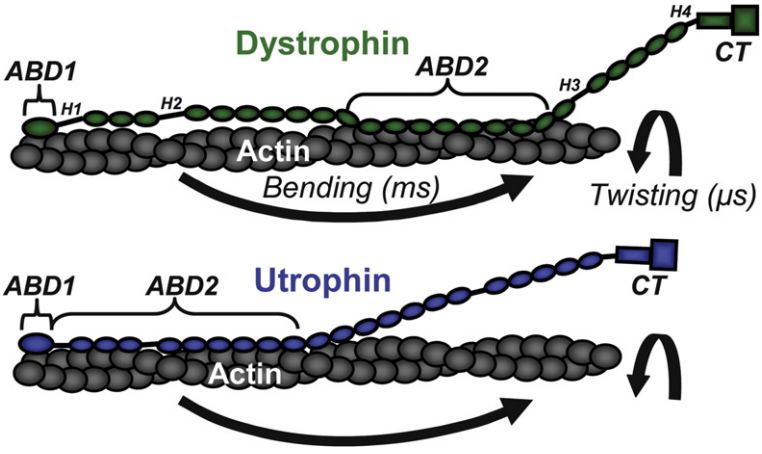

Fig. 1. Diagram of actin filament rotational motions in complexes with dystrophin and utrophin. The homologous structures of the two proteins are indicated schematically. Each has an N-terminal actin-binding domain (ABD1, containing tandem CH domains) and a C-terminal domain (CT) that binds to the sarcolemma, with intervening STRs (ovals) and hinges (H). On the TPA timescale (1–1000 ms), the detected motions are dominated by twisting,[2,3] but the double-helical structure of the actin filament strongly couples its twisting and bending flexibility.[4] The ratio of rotational rate to amplitude, detected by TPA, defines the filament's resilience (see Methods), which is increased by both dystrophin and utrophin.[5]

cytoskeletal organization at key structural regions in striated muscles,[6–8] disabling proper transmission or diffusion of lateral force[9,10] and rendering the muscle susceptible to eccentric contraction damage.[11] Atomic force microscopy studies showed a decrease in myocyte stiffness due to lack of dystrophin.[12] A similar loss in stiffness was observed when cytochalasin D was applied to disrupt the actin cytoskeleton, indicating that the dystrophin–actin interaction plays a central role in maintaining mechanical stability in the muscle cytoskeleton.[12] Our goal is to elucidate the molecular mechanism by which the dystrophin–actin interaction contributes to the molecular mechanics of force transmission and to use this understanding to improve therapeutic strategies.

Utrophin is a 395-kDa dystrophin homolog that is present at the subsarcolemmal region, with functions similar to dystrophin in fetal or regenerating muscle (Fig. 1).[8] As muscle fibers mature, utrophin is replaced by dystrophin,[13–15] but utrophin has been proposed as a viable therapeutic replacement in dystrophin-deficient mice.[16,17] Both proteins contain a highly homologous N-terminal actin-binding domain (ABD1) consisting of tandem CH (*c*alponin *h*omology) motifs, followed by a central domain containing a series of triple-helical spectrin-type repeats (STRs), and a C-terminal (CT) region.[18,19] However, dystrophin and utrophin have distinctly different lateral interactions with actin.[20] Dystrophin's second actin-binding domain (ABD2) is separated from ABD1 by 10 STRs,[21,22] while utrophin's ABD2 is adjacent to ABD1[23,24] (Fig. 1).

We previously used time-resolved phosphorescence anisotropy (TPA) of actin to determine how dystrophin and utrophin affect the structural dynamics of the actin filament (Fig. 1).[5] We showed that the binding of dystrophin or utrophin decreases the amplitude (increases the order) of actin's rotational flexibility while also increasing the rate, both in a highly cooperative manner, thus creating a more resilient complex.[5] We found that utrophin is much more effective than dystrophin in increasing this resilience. The goal of the present study is to understand more clearly how the individual domains of dystrophin and utrophin influence these effects on the resilience of actin.

This goal is important for the rational design of gene therapy for muscular dystrophy, which is currently being developed using recombinant adeno-associated virus vectors. These vectors are size limited; thus, mini- and micro-versions of dystrophin and utrophin have been developed with large deletions of the central STR domains, including all or part of ABD2.[25–28] Since these TRIT (*t*herapeutically *r*elevant *i*nternally *t*runcated) constructs rely on less than a third of the full-length protein, there is a need to evaluate how individual regions in dystrophin and utrophin affect their interaction with actin. The present study applies TPA to further evaluate the effects of isolated regions in dystrophin and utrophin through deletion constructs (Fig. 2).[29,30] Two TRIT constructs, referred to as mini-dystrophin (Mini-Dys in Fig. 2a) and micro-utrophin (Micro-Utr in Fig. 2b), were selected due to the availability of consistent physiological studies in dystrophic (*mdx*) mice.[28,31,32] Additional deletion constructs, with either N- or C-terminal truncations, were engineered to test specific domains within dystrophin and utrophin (Fig. 2).[29,30] Our goal is to use TPA to (a) create a biophysical blueprint that identifies key regions in dystrophin and utrophin required to regulate actin microsecond structural dynamics, (b) investigate why the most promising therapeutic constructs have limited effects on rescuing the dystrophic phenotype in mice, and

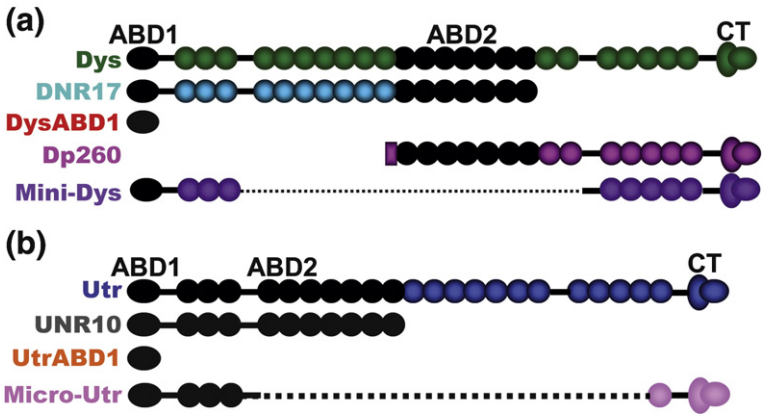

Fig. 2. Constructs evaluated by TPA in this study. (a) Dystrophin. (b) Utrophin. CT, non-actin-binding C-terminal domain. Intervening circles are STRs. Actin-binding domains are depicted in black. This color scheme is used consistently in subsequent figures.

(c) establish TPA as a rapid *in vitro* method for selecting potential therapeutic dystrophin and utrophin constructs according to their ability to mimic the effects of full-length dystrophin on actin dynamics.

Results

Microsecond dynamics of actin in the presence of therapeutically promising mini-dystrophin

To provide motivational context for this study, we begin with the mini-dystrophin construct ("Mini-Dys" in Figs. 2a and 3a).[26,29,30,33] This TRIT (designated DysΔH2-R19 because it lacks the portion from hinge H2 to STR19) is modeled after cases of mild Becker muscular dystrophy, in which up to 46% of the central STR region is missing but the patients can remain ambulatory past 60 years of age.[35–37] Despite the extensive internal deletions, leaving only eight STRs, this construct has shown high efficacy in rescuing the dystrophic phenotype in *mdx* mice.[26,33,38] To compare the TPA results independently of the different actin-binding affinities of the constructs used in this study, we report results as a function of the fractional saturation of binding sites on actin [$\nu = y/B_{max}$; Eq. (7)].[2,5] Direct comparison of the TPA decays when actin binding is 50% saturated ($\nu = 0.5$) shows that Mini-Dys is quite similar to full-length dystrophin (Dys) in its ability to regulate actin structural dynamics (Fig. 3b). Indeed, Mini-Dys decreases the amplitude of rotational dynamics while decreasing the rate (Fig. 3c and d), corresponding to increased actin resilience. This supports our hypothesis that increased actin

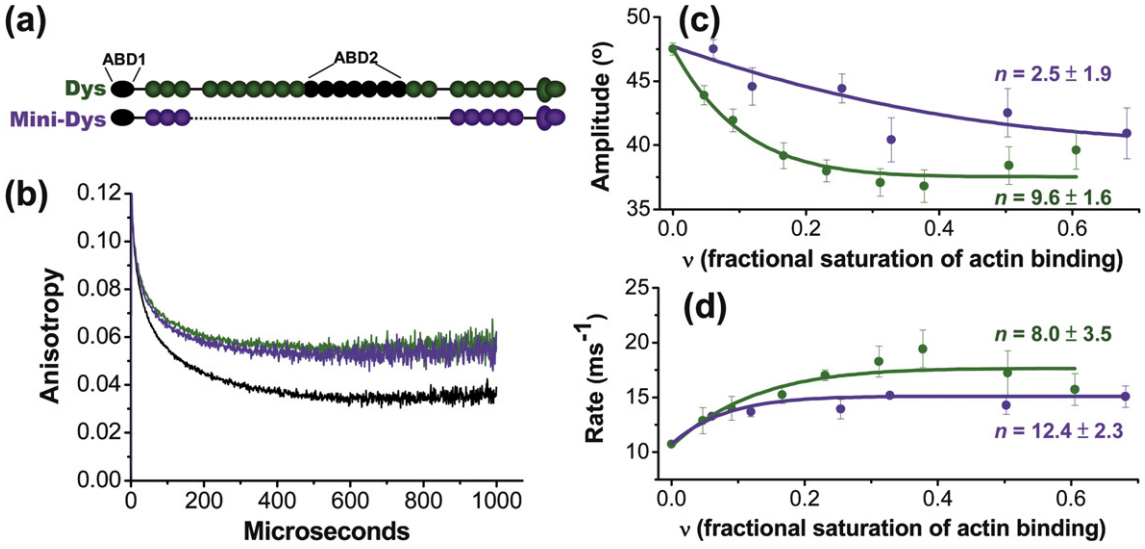

Fig. 3. TPA results comparing dystrophin (Dys) with mini-dystrophin (Mini-Dys). (a) Schematics of Dys and Mini-Dys, with actin-binding domains in black.[20,26,29–33] (b) TPA of actin alone (black) or bound to Dys (green) or Mini-Dys (purple) at 50% saturation of actin binding (n = 0.5). Amplitude (c) and Rate (d) of actin rotational motion from TPA decays, as a function of ν [Eq. (7)]. Curves show fits according to Eq. (8), yielding the degree of cooperativity (n).[3,34]

resilience is a key to the function of dystrophin or its therapeutic surrogates.

The TPA data were analyzed to determine amplitudes and rates [Eqs. (1)–(5)], which were plotted against ν and fitted with Eq. (8). This yielded the cooperativity n, which is the number of actin protomers whose amplitudes and rates are affected by the binding to a single actin protomer (Fig. 3c and d). These plots show that Mini-Dys is less effective than Dys at low ν values, primarily because its effect on amplitude is four times less cooperative ($n=2.5$) than that of Dys ($n=9.6$) (Fig. 3c). This result suggests that Mini-Dys can restore normal actin resilience only at high expression levels, approaching that of Dys in wild-type (wt) mice.

Despite the efficacy of Mini-Dys in rescuing the dystrophic phenotype, its large size causes great challenges for delivery of gene or of protein into muscle using recombinant adeno-associated virus;[32] thus, its development has not progressed beyond small-animal testing.[26,33,38] "Micro" constructs (micro-TRITS, based on utrophin and dystrophin), which have larger internal truncations (typically leaving only four STRs instead of eight), are preferred for large-animal delivery.[26,32,39] To establish a rational basis for the design of micro-TRITs, we used several other deletion constructs (Fig. 2) to investigate systematically the impact of specific regions in dystrophin and utrophin on actin structural dynamics.

Effects of end truncations in dystrophin and utrophin

The constructs of dystrophin containing end truncations (Fig. 4a) were found to retain partial capacity to restrict actin rotational amplitude (Fig. 4b), but they have all lost the capacity to increase actin rotational rate (Fig. 4c). Dp260, which lacks the N-terminal half of Dys (thus lacking ABD1) but retains the second actin-binding domain (ABD2) and the rest of the C-terminal third of Dys, is as cooperative as full-length Dys ($n\sim10$); but DNR17, which contains both actin-binding domains and lacks the C-terminal third, shows much lower cooperativity ($n\sim2$). Thus, the dystrophin C-terminal third, which does not interact directly with actin, appears to play an allosteric role in regulating actin dynamics. The cooperativity of this effect is more pronounced when ABD2 is present (Dp260; Fig. 4b, $n\sim10$) compared with ABD1 alone (mini-dystrophin; Fig. 3c, $n\sim3$). Isolated DysABD1 restricts actin

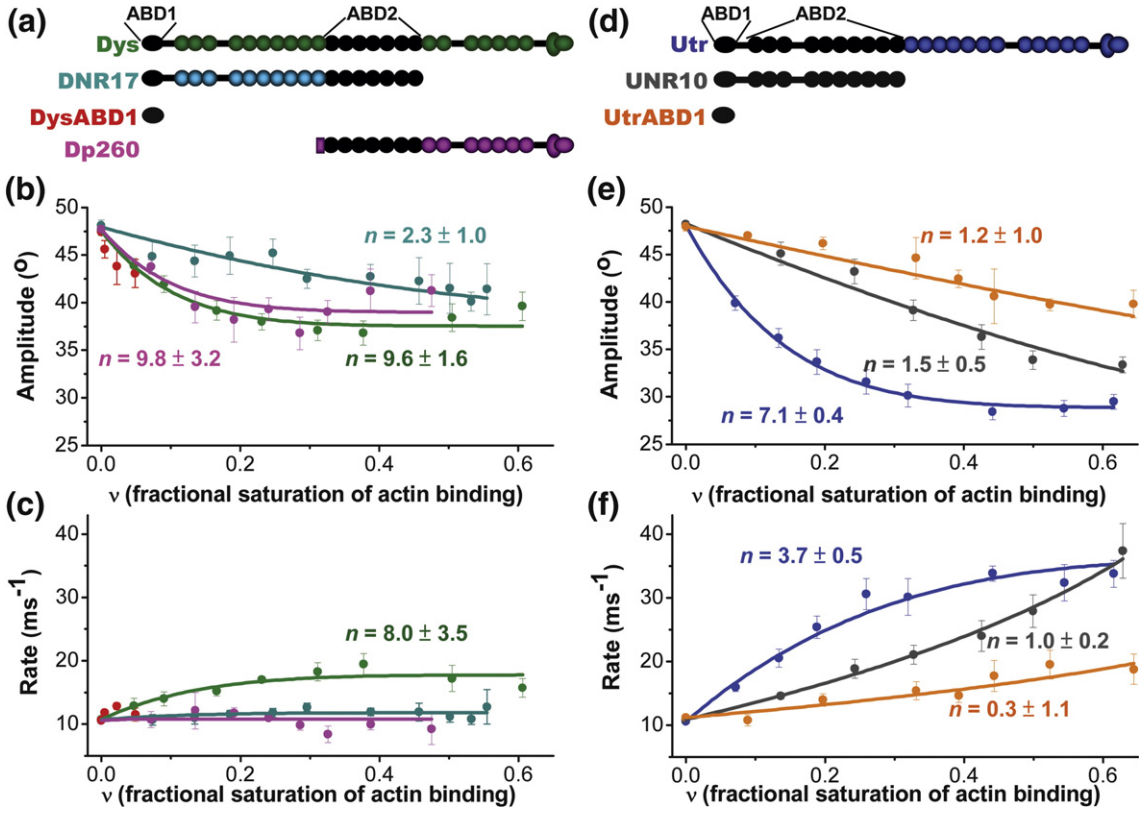

Fig. 4. TPA effects of end-truncation constructs (left, dystrophin; right, utrophin) on actin structural dynamics. In (a) and (d), black regions correspond to actin-binding domains.[20,29,30] Amplitudes (b and e) and Rates (c and f) of actin rotational dynamics are plotted against n [Eq. (7)]. The degree of cooperativity (n) [Eq. (8)] is indicated.[3,34]

rotational amplitude significantly at low ν, but its propensity to bundle actin at higher concentrations[40] prevented a complete analysis.

End truncations in utrophin (Fig. 4d) also decrease its effectiveness on actin dynamics (Fig. 4e and f). UNR10, containing both actin-binding domains but lacking the C-terminal third of Utr, has effects at high ν similar to those of full-length Utr but completely lacks cooperativity (Fig. 4e and f). The isolated ABD1 of Utr is about half as effective as UNR10 and also lacks cooperativity. These results suggest that (1) both actin-binding domains of Utr are important for full regulation of actin dynamics and that (2) the C-terminal portion of Utr appears to determine cooperativity even more clearly than in Dys.

Although deletions in both dystrophin and utrophin decrease their regulation of actin structural dynamics compared with full-length proteins, utrophin constructs retain more effectiveness in enhancing actin resilience. The truncated utrophins retain the capacity to enhance rate substantially, as well as to restrict amplitude (Fig. 4e and f), thus clearly enhancing resilience [Rate/Amplitude; Eq. (5)], while the truncated dystrophins enhanced rate (and hence resilience) only slightly (Fig. 4b and c). These results support the use of a utrophin template for gene therapy designs to enhance actin resilience.

Effect of micro-utrophin on actin dynamics

To test the hypothesis that utrophin is a highly effective template for therapeutic designs, we evaluated a micro-utrophin therapy construct ("Micro-Utr" in Figs. 2 and 5). This micro-TRIT (designated UtrΔR4-21 because the segment from STR4 through STR21 has been deleted, leaving only four STRs) has been previously tested in mouse models.[41] TPA data show that Micro-Utr restricts actin rotational amplitude and increases rate with comparable cooperativity as full-length dystrophin or utrophin (Fig. 5b and c). Although it is not as effective as full-length utrophin, it is more effective than dystrophin at all values of ν.

Effects of dystrophin and utrophin constructs on the resilience of actin

As explained in Methods, resilience of the actin–protein complex is measured from TPA as the ratio of rate to amplitude of actin rotational dynamics, normalized to that of actin alone [Eq. (5)].[5] Figure 6 shows plots of resilience *versus* ν, derived from data

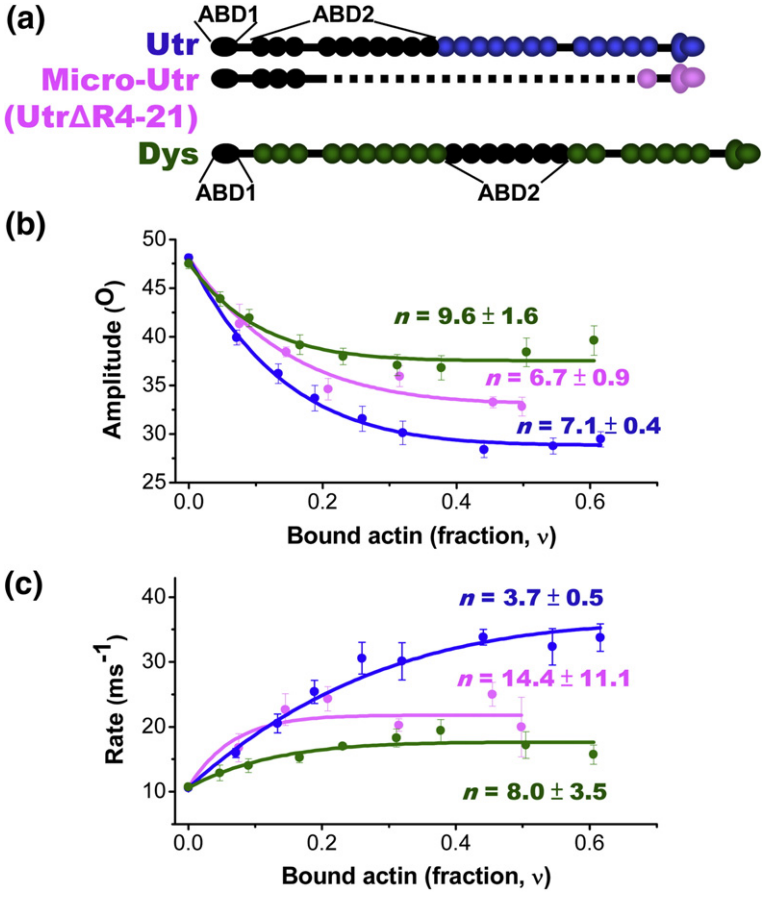

Fig. 5. TPA of actin, showing effects of Micro-Utr, compared with those of full-length Utr and Dys. (a) Schematic of protein structures, with actin-binding domains identified in black. Plots of amplitude (b) and rate (c) of actin rotational motions as a function of actin binding n Curves show fits with [Eq. (8)], yielding cooperativity values n.

in Figs. 3–5. We compared different constructs with regard to their maximum effect on actin resilience (Fig. 6c) and the cooperativity of this effect (Fig. 6d). Resilience was increased by all constructs, but utrophin constructs were consistently more effective than their homologous dystrophin counterparts (e.g., compare Utr with Dys, UNR10 with DNR17, and Micro-Utr with Mini-Dys).

Utrophin's greater capacity than dystrophin, for increasing actin's resilience, correlates well with previous studies of the utrophin's rescue of muscle mechanics in the dystrophin-null *mdx* mouse. Full mechanical function can be restored by upregulation of utrophin at half the level of dystrophin in wt muscle.[17,20,23,33] Similarly, atomic force microscopy analysis of dystrophic myocytes showed that utrophin upregulation can restore cellular stiffness to wt levels at 28% of the wt dystrophin level.[12] This correlation between TPA-measured actin resilience and muscle function also extends to results from physiological tests in *mdx* mice, as discussed below.

Discussion

Deletions in dystrophin and utrophin decrease their effectiveness in regulating actin structural dynamics. However, since utrophin and its constructs are more effective than the dystrophin counterparts, large deletions in utrophin produced structural regulation similar to that of full-length dystrophin, showing great promise for utrophin as a therapeutic surrogate.

The domains of dystrophin

TPA shows that both DNR17 (containing the N-terminal two-thirds of Dys, including both actin-binding domains) and Dp260 (containing the C-terminal one-third of Dys, including ABD2) restrict actin rotational amplitude (Fig. 4b) but have little effect on rate (Fig. 4c) and thus have little effect on resilience (Fig. 6a and c), while

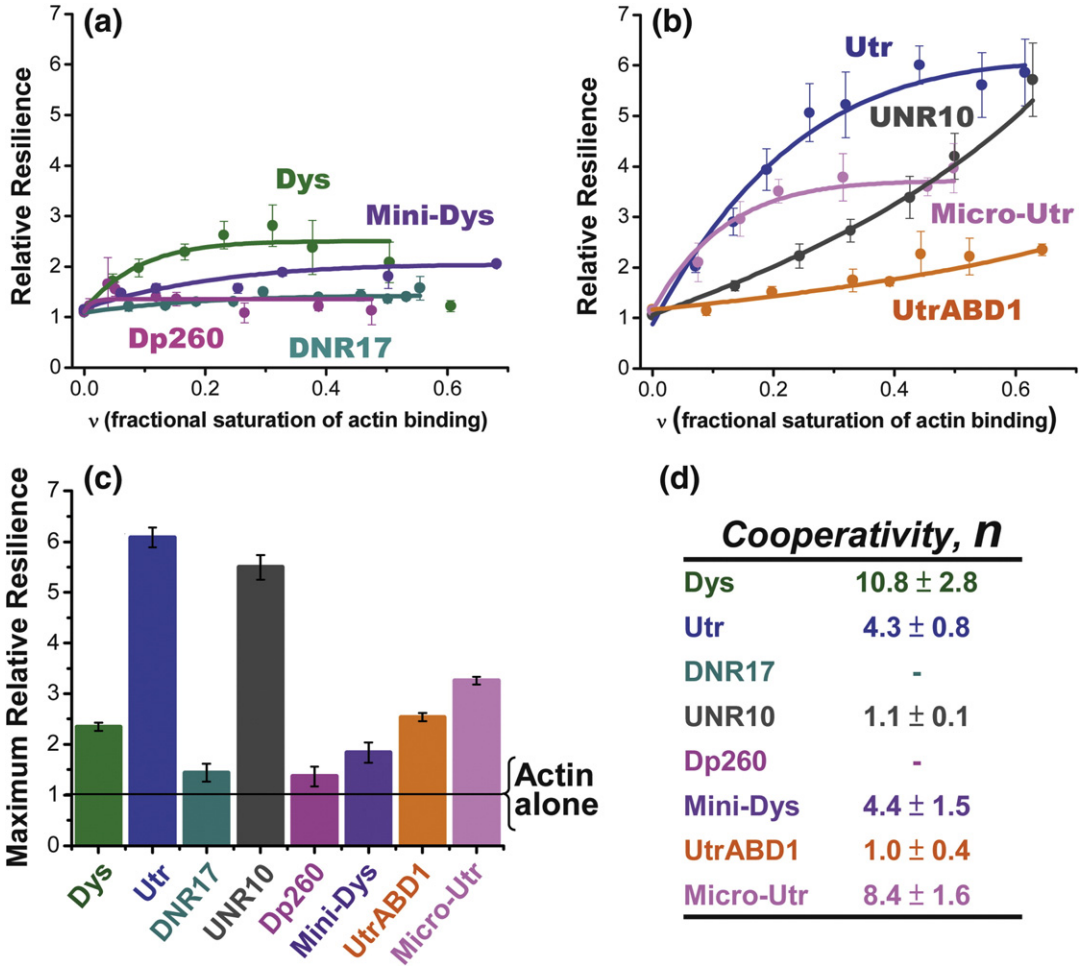

Fig. 6. The resilience of actin, normalized to the value observed for actin alone, in complexes with constructs based on (a) dystrophin and (b) utrophin. Curves show fits with Eq. (8), yielding values for the resilience at saturation (c) and cooperativity (d).

Mini-Dys (containing both N- and C-termini but lacking ABD2) has effects on both amplitude (Fig. 3c) and rate (Fig. 3d), thus enhancing resilience nearly and full-length Dys (Fig. 6a and c). However, the cooperativity of Mini-Dys on actin is less than that of Dys (Fig. 6d), and the highly cooperative restriction of amplitude by Dp260 (Fig. 4b) suggests that the C-terminal region, especially in conjunction with ABD2, is essential for cooperativity in Dys–actin interactions. Thus, the two separated actin-binding domains in dystrophin affect actin structural dynamics with distinctly different but interlacing effects.

The domains of utrophin

Despite their high sequence homology, utrophin's domains have effects on actin structural dynamics that are distinct from those of dystrophin. In general, utrophin's effects are simpler—for example, all four utrophin constructs decrease amplitude to a similar extent that they increase rate (Figs. 4 and 5); thus, it is sufficient to look at the effects on resilience (Rate/Amplitude) (Fig. 6). Another key difference is that utrophin does not require any of its C-terminal half after STR10 to enhance actin's resilience, since the N-terminal UtrABD1 has substantial effects on its own, and UNR10 (lacking the C-terminal half of Utr) has nearly identical effects as full-length Utr at high ν values (Fig. 6b and c). However, neither of these N-terminal constructs (UtrABD1 and UNR10) regulates actin structural dynamics cooperatively (Fig. 6b and d). Since Micro-Utr (which does contain the C-terminus of Utr) shows cooperativity comparable to that of Utr (Fig. 6b and d), it appears that the C-terminal region of Utr, like that of Dys, is essential for conferring cooperativity.

In contrast to dystrophin, the effects of the two actin-binding domains in utrophin appear to be identical and additive. UtrABD1 enhances actin resilience by a factor of 2.3, UNR10 (containing both ABD1 and ABD2 but lacking the C-terminal half) enhances actin resilience by a factor of 5 (Fig. 6), and Micro-Utr (containing ABD1 plus 30% of ABD2) enhances actin resilience by a factor of 2.94 (30% more than UtrABD1). Thus, the regulation of actin structural dynamics by utrophin constructs appears to be simpler and more predictable than that for utrophin constructs. Coupled with the higher efficacy of Utr construct compared with Dys constructs, this result argues for utrophin as a template for therapeutic design.

TPA as a rapid *in vitro* measure of therapeutic efficacy

We surveyed previous physiological studies on *mdx* mice with transgenic expression of dystrophin and utrophin.[17,33] For meaningful comparison of resilience with physiological findings, we considered only studies that tested the mechanical function (specific isometric force) of treated dystrophic muscles, reported levels of expression in the tested muscles, and had tested the animals at the same age. Despite large numbers of studies performed on dystrophic mouse models, few studies meet these standards. However, we found two studies that consistently measured the isometric specific force in diaphragm muscles in *mdx* mice at 3–4 months of age[17,33] (Fig. 7a). These studies included the *Fio* and *Fer* mouse lines that expressed full-length utrophin at 54% and 27% of the endogenous dystrophin level, respectively, in a dystrophin-null background (*mdx*).[17,20,42] A recovery score with regard to the isometric specific force in these mice was calculated based on preclinical standard operating procedures established by TREAT-NMD [Eq. (9)].[43–45] As explained in Methods, resilience values were calculated using data in Fig. 6a and b, to correct for the reported protein expression levels and actin affinities. Correlation plots relating recovery scores of wt muscles (100% recovery with 100% dystrophin) and

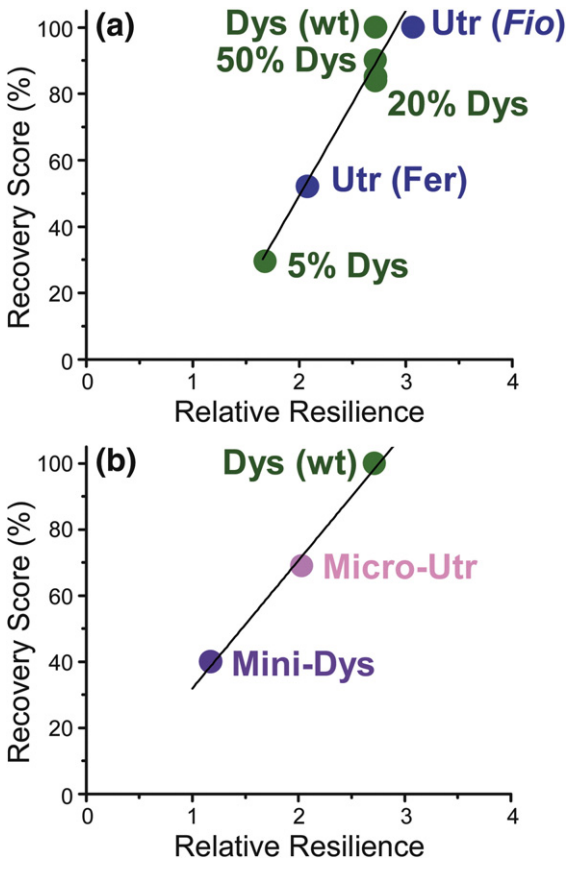

Fig. 7. Correlation of recovery score [Eq. (9)] with actin resilience in *mdx* mice (a) in diaphragm of transgenic mice tested at 3–4 months of age[17,33] and in (b) tibialis anterior.[28,32] Values of Pearson's correlation coefficient (R) [Eq. (10)] are (a) 0.98 and (b) 0.99, respectively.

dystrophic muscles (0% recovery with 0% dystrophin) treated with different levels of dystrophin or utrophin showed a distinctively high correlation to the relative resilience calculated by TPA studies ($R=0.98$). The remarkably linear relationships between the resilience of the actin cytoskeleton and the observed specific force (Fig. 7a) suggest that the measurement of resilience by TPA is a potentially useful *in vitro* predictor of the therapeutic efficacy of dystrophin and utrophin constructs.

Our measured resilience also demonstrated excellent correlation with mechanical restoration of dystrophic muscles treated with Mini-Dys[32] and Micro-Dys[28,41] (Fig. 7b, $R=0.99$). Although the micro-utrophin construct demonstrated a larger effect on increasing actin resilience compared to wt dystrophin at saturating levels (Fig. 6c), the *mdx* study did not achieve saturating expression levels in the tested muscles.[28] As a result, the resulting relative resilience calculated based on the level of micro-utrophin expression reported and on our data (Fig. 6a and b) was lower than that expected for Dys (wt), in which actin is saturated with full-length dystrophin. This further supports the use of TPA as a rapid *in vitro* method to screen proposed gene therapy constructs for potential therapeutic efficacy.

Our results suggest the feasibility of using utrophin as a therapeutic surrogate. Figure 6c shows that utrophin constructs consistently provided higher resilience compared with dystrophin constructs. Even Micro-Utr provided higher resilience compared with full-length dystrophin, despite extensive internal deletions. Thus, the same level of resilience can be achieved with lower concentrations of utrophin constructs compared with dystrophin constructs. This is consistent with the finding that expression of full-length utrophin at half the concentration of wt dystrophin was sufficient to fully restore muscle mechanics.[17] Since improving the transfection efficacy of these therapeutic constructs is still an ongoing pursuit, our data suggest that it would be most beneficial to use a utrophin-derived construct. Coupled with possible immunogenicity in dystrophin-derived therapeutic constructs,[46] these results argue for the use of utrophin as a template for gene therapy designs.

Conclusion

We have used TPA to draw a biophysical blueprint of dystrophin and utrophin regarding their effects on actin structural dynamics and resilience. The domains of dystrophin and utrophin have different effects on actin, despite their high structural homology. Utrophin constructs are generally more robust in making actin resilient, despite large deletions. Compared with dystrophin constructs, utrophin constructs are more effective in enhancing actin resilience, and the effects of their domains on actin resilience are simpler and more independent, facilitating rational design. We find a strong correlation between resilience of actin–protein complexes and functional restoration reported from previous studies in *mdx* mice. We propose to use TPA as a rapid *in vitro* screening method for designing and testing the next generation of gene therapy constructs for muscular dystrophy.

Methods

Protein preparation

Larger dystrophin and utrophin constructs including DNR17, UNR10, Dp260, and DysΔH2-R19 were expressed using Sf9 insect cells infected with high-titer recombinant N-terminal FLAG tags.[26,29,30] FLAG-Micro-Utr was engineered by recombinant PCR using FLAG-Utr cDNA as a template with identical primers as previously described.[28] Proteins were purified by FLAG affinity chromatography and dialyzed against two changes of phosphate-buffered saline (pH 7.5) to remove excess FLAG peptide. DysABD1 and UtrABD1 are expressed in *Escherichia coli* BL21 AI cell line and purified using a cation exchange (HiTrap SP XL; GE) for DysABD1 and an anion exchange (HiTrap Q XL; GE) for UtrABD1 followed by a size-exclusion column (Sephadex S200; GE). Proteins were concentrated in Millipore Amicon ultracentrifuge-based concentrators with cutoffs of either 100 kDa or 10 kDa depending on protein molecular mass. Concentrations were determined by Bradford protein assay with a bovine serum albumin standard.

Time-resolved phosphorescence anisotropy

Actin preparation and labeling with phosphorescent erythrosine iodoacetamide (ErIA) (Anaspec) was as described in Ref. [5]. Phalloidin-stabilized ErIA-actin was diluted in U/D buffer [100 mM $NaCl_2$, 2 mM $MgCl_2$, 0.2 mM ATP, 1 mM DTT, and 10 mM Tris (pH 7.5)] to 1 μM. Increasing concentrations of dystrophin and utrophin constructs were added to bind to 1 μM ErIA-actin. Oxygen removing system containing of glucose oxidase (55 μg/ml), catalase (36 μg/ml), and glucose (45 μg/ml) was added to the sample prior to each experiment and incubated for 5 min to prevent photobleaching.[47,48] The phosphorescent dye is excited at 532 nm with a vertically polarized 1.2-ns laser pulse from a FDSS 532-150 laser (CryLas) with a 100-Hz repetition rate. Emission was detected through a 670-nm-glass cutoff filter (Corion) using a photomultiplier (R928; Hamamatsu) and a transient digitizer (CompuScope 14100; GaGe) with a resolution of 1 μs per channel. Time-resolved anisotropy is defined by

$$r(t)=[I_v(t)-GI_h(t)]/[I_v(t)+2GI_h(t)] \quad (1)$$

where $I_v(t)$ and $I_h(t)$ are the vertically and horizontally polarized components of the detected phosphorescent

emission, using a single detector at 90° and a rotating sheet polarizer alternating between the two orientations every 500 laser pulses. G is a correction factor calibrated by detection of the signal with horizontally polarized excitation and correcting so that the anisotropy is zero. TPA experiments were recorded with 30 cycles, each consisting of 500 pulses in each polarization.

Anisotropy decays were analyzed by fitting to the sum of two exponential terms.[2,5] Results were validated by comparison of residuals and chi-squared values of the fits at one, two, and three exponential terms, with the best fit consistently requiring two exponential terms.

$$r(t)=r_1\exp(-t/\phi_1)+r_2\ \exp(-t/\phi_2)+r_\infty \tag{2}$$

The overall angular amplitude of rotational motion was defined as the radius of a cone calculated from the wobble-in-cone model.[2]

$$\text{Amplitude} = \theta_c = \cos^{-1}\left[-0.5+\left\{0.5\left(1+8[r_\infty/r_0]^{1/2}\right)\right\}^{1/2}\right] \tag{3}$$

Thus, a maximally flexible actin filament would exhibit a final anisotropy value of $r_\infty=0$, yielding, and a cone angle of $\theta_c=90°$, and a rigid filament would have $r_\infty=r_0$ (no decay) and $\theta_c=0°$ (no detectable rotation).

The mean rate of actin filament rotational motions was defined as the inverse of the mean correlation time:

$$\text{Rate}=(r_1+r_2)/(\phi_1 r_1+\phi_2 r_2) \tag{4}$$

Resilience is defined as the maximum amount of elastic energy per unit volume that can be stored without large structural distortions to the protein complex.[49] Highly resilient polymers can recover quickly from deformations. During this process, the system stores mechanical energy from deformation as elastic energy.[50] Resilience of the actin-bound complex is determined from TPA as:

$$\text{Resilience} = \text{Rate}/\text{Amplitude} \tag{5}$$

where Amplitude is calculated from Eq. (3), and Rate is calculated from Eq. (4).[5] The plotted resilience values of Fig. 6 are "Relative Resilience," normalized to the value observed for actin alone in the same study.

TPA-derived parameters (Amplitude, Rate, or Resilience) are plotted against the fractional saturation of actin binding (ν=bound protein molecules per binding site on actin). These ν values were determined from actin-binding assays of dystrophin and utrophin constructs using high-speed co-sedimentation.[5,51] Varying concentrations of dystrophin or utrophin constructs were added to 6 μM labeled actin, incubated for 30 min at 20 °C, and centrifuged at 100,000*g* for 20 min. The resulting pellets and supernatants were analyzed by SDS-PAGE to determine the concentrations of free and actin-bound protein. Then K_d (dissociation constant in micromolars) and B_{max} (number of protein-binding sites per actin protomer) were determined by fitting the data with

$$y = B_{max}[P]/(K_d+[P]) \tag{6}$$

where y is the moles of bound protein per mole of actin, and [P] is the concentration of free protein. Thus, B_{max} and K_d were determined for each construct. In TPA experiments, the concentration of free protein [P] was not known; thus, y was calculated from

$$y = B_{max}\left\{[P_T]+B_{max}+K_d - \left[([P_T]+B_{max}+K_d)^2-4[P_T]B_{max}\right]^{1/2}\right\}/2B_{max}$$
$$\nu = y/B_{max} \tag{7}$$

where $[P_T]$ is the total concentration of protein added to labeled actin, and ν is the fractional saturation of actin-binding sites used in the horizontal axes of Figs. 3–6.

Cooperativity

The degree of cooperativity was determined by fitting the plot of rotational Amplitude [Eq. (3)], Rate [Eq. (4)], or Resilience [Eq. (5)] *versus* ν [Eq. (7)] to the expression:[3,34]

$$X(\nu)=X_{max}-(X_{max}-X_0)(1-\nu)^n \tag{8}$$

where $X(\nu)$ is the observed value (Amplitude, Rate, or Resilience), X_0 is the value for actin only ($\nu=0$), X_{max} is the value when actin is fully saturated ($\nu=1$), $\nu=y/B_{max}$ [Eq. (7)] is the fraction of actin sites occupied by added protein, and n is the degree of cooperativity in the system, that is, the number of actin protomers affected by the binding of a single actin protomer. In other words, the number of actin protomers affected dynamically by the binding of one protein molecule in each experiment is n B_{max}.

Correlation with preclinical data

In order to correlate resilience, as measured by TPA, with specific force measured in mice (Fig. 7), we normalized resilience according to the level of expressed constructs, relative to dystrophin in the wt mouse, reported from each mouse study.[17,28,32] The concentration of dystrophin in wt mouse muscle was calculated from previous reports.[20,52] Dystrophin comprises 0.026% of total muscle protein,[20] which amounts to 0.12 μM with a cellular density of 0.2 g/ml.[52] We assume a sarcolemmal surface area-to-cell volume ratio of 0.103 $\mu m^2/\mu m^3$[53] and a length of 120 nm in the z-dimension (length of the dystrophin molecule).[23] Thus, the estimated local concentration of dystrophin is 9.9 μM in the wt mouse. Similarly, the concentration of cytoskeletal γ-actin at the subsarcolemmal region (using a total γ-actin concentration of 0.20 μM reported in the whole cell)[52] was calculated to be 16 μM. Since one dystrophin molecule interacts with 27 actin protomers with submicromolar affinity,[20] we assume that the fraction of dystrophin-decorated actin at the costamere is 1 ($\nu=1$). To normalize the relative resilience of each construct to the reported percentage of expression levels in each study, we use Eq. (7) to calculate the fractional saturation ν for each construct, based on their respective K_d and B_{max} values.[20] The resilience of the actin cytoskeleton was determined from this value of ν, using the plots in Fig. 6a and b.

To compare the mechanical function of treated muscles across studies, we used the preclinical standard operating procedure to calculate a recovery score, based on measurements of isometric specific force:[43–45]

$$\text{Recovery Score} = (\text{treated} - \text{untreated})/(\text{wt} - \text{untreated}) \tag{9}$$

where Pearson's correlation coefficient (R) was calculated from

$$R = \frac{1}{m}\sum_{i=1}^{m}\left(\frac{x_i - \bar{x}}{\sigma_x}\right)\left(\frac{y_i - \bar{y}}{\sigma_y}\right) \tag{10}$$

where m is the number of samples, and x_i and y_i are the values of specific force and actin resilience. x and y are the mean values, and σ_x and σ_y are the standard deviations.

Acknowledgements

TPA experiments were performed at the Biophysical Spectroscopy Facility, University of Minnesota, and at Muscular Dystrophy Core Laboratories at the University of Minnesota supported by National Institutes of Health (NIH) grant P30-AR0507220. Excellent computational resources were provided by the Minnesota Supercomputing Institute. Special thanks to Octavian Cornea for assistance with manuscript preparation and submission and Dawn Lowe for useful discussions. We also thank Hanke Heun-Johnson for her technical assistance in engineering the FLAG-Micro-Utr construct. This study was supported by NIH grants AR032961, AR057220 Core C, and AG026160 (to D.D.T.); Muscular Dystrophy Association grant 4322 (to D.D.T.); NIH grants AR007612 and AR042423 (to J.M.E.); and NIH grant F30AG034033 (to A.Y.L.).

References

1. Ervasti, J. M. & Campbell, K. P. (1993). Dystrophin and the membrane skeleton. *Curr. Opin. Cell Biol.* **5**, 82–87.
2. Prochniewicz, E., Zhang, Q., Howard, E. C. & Thomas, D. D. (1996). Microsecond rotational dynamics of actin: spectroscopic detection and theoretical simulation. *J. Mol. Biol.* **255**, 446–457.
3. Prochniewicz, E., Janson, N., Thomas, D. D. & De la Cruz, E. M. (2005). Cofilin increases the torsional flexibility and dynamics of actin filaments. *J. Mol. Biol.* **353**, 990–1000.
4. De La Cruz, E. M., Roland, J., McCullough, B. R., Blanchoin, L. & Martiel, J. L. (2010). Origin of twist-bend coupling in actin filaments. *Biophys. J.* **99**, 1852–1860.
5. Prochniewicz, E., Henderson, D., Ervasti, J. M. & Thomas, D. D. (2009). Dystrophin and utrophin have distinct effects on the structural dynamics of actin. *Proc. Natl Acad. Sci. USA*, **106**, 7822–7827.
6. Paul, A., Sheard, P., Kaufman, S. & Duxson, M. (2002). Localization of a7 integrins and dystrophin suggests potential for both lateral and longitudinal transmission of tension in large mammalian muscles. *Cell Tissue Res.* **308**, 255–265.
7. Cohn, R. D. & Campbell, K. P. (2000). Molecular basis of muscular dystrophies. *Muscle Nerve*, **23**, 1456–1471.
8. Blake, D. J., Weir, A., Newey, S. E. & Davies, K. E. (2002). Function and genetics of dystrophin and dystrophin-related proteins in muscle. *Physiol. Rev.* **82**, 291–329.
9. Street, S. F. (1983). Lateral transmission of tension in frog myofibers: a myofibrillar network and transverse cytoskeletal connections are possible transmitters. *J. Cell. Physiol.* **114**, 346–364.
10. Ramaswamy, K. S., Palmer, M. L., van der Meulen, J. H., Renoux, A., Kostrominova, T. Y., Michele, D. E. & Faulkner, J. A. (2011). Lateral transmission of force is impaired in skeletal muscles of dystrophic mice and very old rats. *J. Physiol.* **589**, 1195–1208.
11. Petrof, B. J., Shrager, J. B., Stedman, H. H., Kelly, A. M. & Sweeney, H. L. (1993). Dystrophin protects the sarcolemma from stresses developed during muscle contraction. *Proc. Natl Acad. Sci. USA*, **90**, 3710–3714.
12. Puttini, S., Lekka, M., Dorchies, O. M., Saugy, D., Incitti, T., Ruegg, U. T. *et al.* (2008). Gene-mediated restoration of normal myofiber elasticity in dystrophic muscles. *Mol. Ther.* **17**, 19–25.
13. Takemitsu, M., Ishiura, S., Koga, R., Kamakura, K., Arahata, K., Nonaka, I. & Sugita, H. (1991). Dystrophin-related protein in the fetal and denervated skeletal muscles of normal and mdx mice. *Biochem. Biophys. Res. Commun.* **180**, 1179–1186.
14. Rafael, J. A. & Brown, S. C. (2000). Dystrophin and utrophin: genetic analyses of their role in skeletal muscle. *Microsc. Res. Tech.* **48**, 155–166.
15. Lin, S. & Burgunder, J. M. (2000). Utrophin may be a precursor of dystrophin during skeletal muscle development. *Dev. Brain Res.* **119**, 289–295.
16. Tinsley, J. M., Potter, A. C., Phelps, S. R., Fisher, R., Trickett, J. I. & Davies, K. E. (1996). Amelioration of the dystrophin phenotype of *mdx* mice using a truncated utrophin transgene. *Nature*, **384**, 349–353.
17. Tinsley, J., Deconinck, N., Fisher, R., Kahn, D., Phelps, S., Gillis, J. M. & Davies, K. (1998). Expression of full-length utrophin prevents muscular dystrophy in *mdx* mice. *Nat. Med.* **4**, 1441–1444.
18. Koenig, M., Monaco, A. P. & Kunkel, L. M. (1988). The complete sequence of dystrophin predicts a rod-shaped cytoskeletal protein. *Cell*, **53**, 219–228.
19. Hoffman, E. P., Brown, R. H., Jr. & Kunkel, L. M. (1987). Dystrophin: the protein product of the Duchenne muscular dystrophy locus. *Cell*, **51**, 919–928.
20. Rybakova, I. N., Humston, J. L., Sonnemann, K. J. & Ervasti, J. M. (2006). Dystrophin and utrophin bind actin through distinct modes of contact. *J. Biol. Chem.* **281**, 9996–10001.

21. Amann, K. J., Renley, B. A. & Ervasti, J. M. (1998). A cluster of basic repeats in the dystrophin rod domain binds F-actin through an electrostatic interaction. *J. Biol. Chem.* **273**, 28419–28423.
22. Ervasti, J. M. (2007). Dystrophin, its interactions with other proteins, and implications for muscular dystrophy. *Biochim. Biophys. Acta*, **1772**, 108–117.
23. Rybakova, I. N., Patel, J. R., Davies, K. E., Yurchenco, P. D. & Ervasti, J. M. (2002). Utrophin binds laterally along actin filaments and can couple costameric actin with sarcolemma when overexpressed in dystrophin-deficient muscle. *Mol. Biol. Cell*, **13**, 1512–1521.
24. Rybakova, I. N. & Ervasti, J. M. (2005). Identification of spectrin-like repeats required for high affinity utrophin–actin interaction. *J. Biol. Chem.* **280**, 23018–23023.
25. Fisher, K. J., Jooss, K., Alston, J., Yang, Y., Haecker, S. E., High, K. *et al.* (1997). Recombinant adeno-associated virus for muscle directed gene therapy. *Nat. Med.* **3**, 306–312.
26. Harper, S. Q., Hauser, M. A., DelloRusso, C., Duan, D., Crawford, R. W., Phelps, S. F. *et al.* (2002). Modular flexibility of dystrophin: implications for gene therapy of Duchenne muscular dystrophy. *Nat. Med.* **8**, 253–261.
27. Odom, G. L., Gregorevic, P., Allen, J. M., Finn, E. & Chamberlain, J. S. (2008). Microutrophin delivery through rAAV6 increases lifespan and improves muscle function in dystrophic dystrophin/utrophin-deficient mice. *Mol. Ther.* **16**, 1539–1545.
28. Sonnemann, K. J., Heun-Johnson, H., Turner, A. J., Baltgalvis, K. A., Lowe, D. A. & Ervasti, J. M. (2009). Functional substitution by TAT-utrophin in dystrophin-deficient mice. *PLoS Med.* **6**, e1000083.
29. Henderson, D. M., Belanto, J. J., Li, B., Heun-Johnson, H. & Ervasti, J. M. (2011). Internal deletion compromises the stability of dystrophin. *Hum. Mol. Genet.* **20**, 2955–2963.
30. Henderson, D. M., Lin, A. Y., Thomas, D. D. & Ervasti, J. M. (2012). The carboxy-terminal third of dystrophin enhances actin binding activity. *J. Mol. Biol.* **416**, 414–424.
31. Warner, L. E., DelloRusso, C., Crawford, R. W., Rybakova, I. N., Patel, J. R., Ervasti, J. M. & Chamberlain, J. S. (2002). Expression of Dp260 in muscle tethers the actin cytoskeleton to the dystrophin–glycoprotein complex and partially prevents dystrophy. *Hum. Mol. Genet.* **11**, 1095–1105.
32. Odom, G. L., Gregorevic, P., Allen, J. M. & Chamberlain, J. S. (2011). Gene therapy of mdx mice with large truncated dystrophins generated by recombination using rAAV6. *Mol. Ther.* **19**, 36–45.
33. Phelps, S. F., Hauser, M. A., Cole, N. M., Rafael, J. A., Hinkle, R. T., Faulkner, J. A. & Chamberlain, J. S. (1995). Expression of full-length and truncated dystrophin mini-genes in transgenic mdx mice. *Hum. Mol. Genet.* **4**, 1251–1258.
34. Prochniewicz, E., Zhang, Q., Janmey, P. A. & Thomas, D. D. (1996). Cooperativity in F-actin: binding of gelsolin at the barbed end affects structure and dynamics of the whole filament. *J. Mol. Biol.* **260**, 756–766.
35. England, S. B., Nicholson, L. V. B., Johnson, M. A., Forrest, S. M., Love, D. R., Zubrzycka-Gaarn, E. E. *et al.* (1990). Very mild muscular dystrophy associated with the deletion of 46% of dystrophin. *Nature*, **343**, 180–182.
36. Yazaki, M., Yoshida, K., Nakamura, A., Koyama, J., Nanba, T., Ohori, N. & Ikeda, S. i. (1999). Clinical characteristics of aged Becker muscular dystrophy patients with onset after 30 years. *Eur. Neurol.* **42**, 145–149.
37. Matsumura, K., Burghes, A. H., Mora, M., Tomé, F. M., Morandi, L., Cornello, F. *et al.* (1994). Immunohistochemical analysis of dystrophin-associated proteins in Becker/Duchenne muscular dystrophy with huge in-frame deletions in the NH2-terminal and rod domains of dystrophin. *J. Clin. Invest.* **93**, 99–105.
38. Wang, B., Li, J. & Xiao, X. (2000). Adeno-associated virus vector carrying human minidystrophin genes effectively ameliorates muscular dystrophy in mdx mouse model. *Proc. Natl Acad. Sci.* **97**, 13714–13719.
39. Wang, Z., Chamberlain, J. S., Tapscott, S. J. & Storb, S. (2009). Gene therapy in large animal models of muscular dystrophy. *ILAR J.* **50**, 187–198.
40. Orlova, A. & Egelman, E. H. (1993). A conformational change in the actin subunit can change the flexibility of the actin filament. *J. Mol. Biol.* **232**, 334–341.
41. Call, J. A., Ervasti, J. M. & Lowe, D. A. (2011). TAT-microutrophin mitigates the pathophysiology of dystrophin and utrophin double-knockout mice. *J. Appl. Physiol.* **111**, 200–205.
42. Rybakova, I. N., Patel, J. R. & Ervasti, J. M. (2000). The dystrophin complex forms a mechanically strong link between the sarcolemma and costameric actin. *J. Cell Biol.* **150**, 1209–1214.
43. Gillis, J. M. (2008). *The recovery score of evaluated therapy efficiency in NMD: a common, quantitative and comparative scoring system.* 1st edit., vol. 2008, George Carlson, Washington, DC, USA.
44. Deconinck, N., Tinsley, J., Backer, F. D., Fisher, R., Kahn, D., Phelps, S. *et al.* (1997). Expression of truncated utrophin leads to major functional improvements in dystrophin-deficient muscles of mice. *Nat. Med.* **3**, 1216–1221.
45. Jean-Marie, G. (2002). Multivariate evaluation of the functional recovery obtained by the overexpression of utrophin in skeletal muscles of the *mdx* mouse. *Neuromuscular Disord.* **12**, S90–S94; Supplement 1.
46. Mendell, J. R., Campbell, K., Rodino-Klapac, L., Sahenk, Z., Shilling, C., Lewis, S. *et al.* (2010). Dystrophin immunity in Duchenne's muscular dystrophy. *N. Engl. J. Med.* **363**, 1429–1437.
47. Prochniewicz, E., Walseth, T. F. & Thomas, D. D. (2004). Structural dynamics of actin during active interaction with myosin: different effects of weakly and strongly bound myosin heads. *Biochemistry*, **43**, 10642–10652.
48. Eads, T. M., Thomas, D. D. & Austin, R. H. (1984). Microsecond rotational motions of eosin-labeled myosin measured by time-resolved anisotropy of absorption and phosphorescence. *J. Mol. Biol.* **179**, 55–81.
49. Availone, E. A., Baumeister, T., III & Sadegh, A. M. (2007). *Marks' Standard Handbook for*

Mechanical Engineers, 11th edit. McGraw-Hill, New York, NY.
50. Gosline, J., Lillie, M., Carrington, E., Guerette, P., Ortlepp, C. & Savage, K. (2002). Elastic proteins: biological roles and mechanical properties. *Philos. Trans. R. Soc., B*, **357**, 121–132.
51. Rybakova, I. N., Amann, K. J. & Ervasti, J. M. (1996). A new model for the interaction of dystrophin with F-actin. *J. Cell Biol.* **135**, 661–672.
52. Hanft, L. M., Rybakova, I. N., Patel, J. R., Rafael-Fortney, J. A. & Ervasti, J. M. (2006). Cytoplasmic γ-actin contributes to a compensatory remodeling response in dystrophin-deficient muscle. *Proc. Natl Acad. Sci. USA*, **103**, 5385–5390.
53. Bers, D. M. (1991). *Excitation–Contraction Coupling and Cardiac Contractile Force.* Kluwer Academic Publishers, Dordrecht, The Netherlands.